Role of heparanase 2 (Hpa2) in gastric cancer

JingJing Liu
Third Military Medical University, Chongqing
Ibrahim Knani
Technion Israel Institute of Technology
Miriam Gross-Cohen
Technion Israel Institute of Technology
Hu Jiaxi
Third Military Medical University: Army Medical University
Wang Sumin
Third Military Medical University: Army Medical University
Tang Li
Third Military Medical University: Army Medical University
Neta Ilan (netailan@technion.ac.il)
Technion Israel Institute of Technology https://orcid.org/0000-0003-3549-4904
Shiming Yang
Third Military Medical University: Army Medical University
Israel Vlodavsky
Technion Israel Institute of Technology

Research Article

Keywords: Heparanase 2, gastric cancer, stress, AMPK

Posted Date: March 23rd, 2021

DOI: https://doi.org/10.21203/rs.3.rs-336270/v1

Abstract

Background

Heparanase is highly implicated in tumor metastasis due to its capacity to cleave heparan sulfate (HS) and, consequently, remodel the extracellular matrix (ECM) underlying epithelial and endothelial cells. In striking contrast, only little attention was given to its close homolog, heparanase 2 (Hpa2), possibly because it lacks HS-degrading activity typical of heparanase.

Methods

We combined clinical, in vivo and in vitro studies to reveal the role of Hpa2 in gastric cancer.

Results

Here, we report that gastric cancer patients exhibiting high levels of Hpa2 survive longer. Similarly, mice administrated with gastric carcinoma cells engineered to over-express Hpa2 produced smaller tumors and survived longer than mice administrated with control cells. This was associated with increased phosphorylation of AMP-activated protein kinase (AMPK), a kinase that is situated at the center of a tumor suppressor network known to attenuate the growth of various types of cancer including gastric cancer. We also found that MG132, an inhibitor of the proteasome that results in proteotoxic stress, prominently enhances Hpa2 expression. Notably, Hpa2 induction by MG132 appeared to be mediated by AMPK, and AMPK was found to induce the expression of Hpa2, thus establishing a loop that feeds itself where Hpa2 enhances AMPK phosphorylation that, in turn, induces Hpa2 expression, leading to attenuation of gastric tumorigenesis.

Conclusions

These results indicate that high levels of Hpa2 in some tumors but not in others are due to stress conditions that tumors often experience due to their high rates of cell proliferating, high metabolic demands, and changes in the tumor microenvironment. This increase in Hpa2 levels by the stressed tumors appears critically important for the patient's outcome.

Background

Gastric adenocarcinoma is the fifth most commonly diagnosed cancer and the third leading cause of cancer-related death worldwide; over a million new cases of gastric cancer are diagnosed each year (2). Despite the use of multiple treatment modalities, including surgery, combined with radiation therapy, chemotherapy, or targeted chemo-immune therapy, the disease often progresses, relapses, or metastasizes and has a 5-year survival rate of less than 35% overall, and only 2% for cases of peritoneal metastases (3). Thus, better understanding of the disease and the development of new treatment modalities are required to offer patients more effective treatment options.

Heparanase is an endo-β-D-glucuronidase proficient in cleaving heparan sulfate (HS) side chains of heparan sulfate proteoglycans (HSPG). These macromolecules are highly abundant in the extracellular matrix (ECM) underlying epithelial and endothelial cells, where they bind the major protein constituents of the ECM (i.e., laminin, fibronectin, collagen-IV, etc.). This HS-bridge between ECM components assists in establishing a three-dimensional, non-soluble, thick matrix that provides structural support and biochemical cues to many types of cells (4–6). Cleavage of HS by heparanase thus results in remodeling of the ECM, most notably associating with sprouting of new blood vessels (angiogenesis) and cell dissemination coupled with tumor metastasis and transmigration of immune cells (7–9). Also, heparanase can release a wide variety of enzymes, growth factors, cytokines and chemokines that are bound to HS as a storage depot (10), converting them into active biological mediators. Heparanase is, therefore, considered pro-tumorigenic in many types of cancers, and patients that exhibit high levels of heparanase survive less time than patients with low levels of heparanase (7, 11, 12), thus encouraging the development of heparanase inhibitors. Few such inhibitors are currently under clinical evaluation (13, 14). Similar considerations are also noted in gastric cancer (15). Meta-analyses revealed that high expression of heparanase mRNA and protein are correlated with increased depth of invasion, lymph node metastasis, tumor size and TNM stage (16), associating with poor prognosis (17).

Unlike heparanase, the role of heparanase 2 (Hpa2), a close homolog of heparanase (18), in cancer is largely unknown. Decreased levels of Hpa2 in several types of cancer vs adjacent normal tissues (19) suggest that this protein functions to attenuate tumorigenesis, as was shown in head and neck cancer (20). However, its role and mode of action in gastric cancer have not been elucidated yet. Here, we report that gastric cancer patients exhibiting high levels of Hpa2 survive longer. Similarly, mice administrated with gastric carcinoma cells engineered to overexpress Hpa2 produced smaller tumors and survived longer than mice administrated with control cells. These beneficial effects were found to associate with increased phosphorylation of AMP-activated protein kinase (AMPK) that play an instrumental role in cell metabolism. Also, AMPK is situated at the center of a tumor suppressor network known to attenuate the growth of many types of cancer including gastric cancer (1). Interestingly, AMPK was found to induce the expression of Hpa2, thus establishing a loop that feeds itself where Hpa2 enhances AMPK phosphorylation that, in turn, induces Hpa2 expression, leading to attenuation of gastric tumorigenesis.

Materials And Methods

Gastric tissue arrays. Two gastric tissue arrays were purchased from Outdo Biotech Co., Ltd. (http://www.superchip.com.cn/) including 90 (HStma180Su09) and 98 (HStmA180Su15) gastric carcinoma patients and adjacent normal gastric tissue. The array provided clinicopathological information in accordance with the American Joint Committee on Cancer (AJCC) 2010, including TNM classification and overall survival data. Gastric carcinoma tissue array (ST2084), was also purchased from US Biomax (Rockville, MD).

Cells and cell culture. Human AGS, BGC-832, MKN-45, SGC-7901, and MGC-803 gastric carcinoma and mouse Lewis lung carcinoma (LLC) cells have been described previously (21–23) and were grown in

Dulbecco's modified Eagle's medium (Biological Industries, Beit Haemek, Israel) supplemented with 10% FCS and antibiotics.

Antibodies and reagents. Anti-Hpa2 antibody (#58) has been described previously (20). Anti-phospho-acetyl CoA carboxylase (ACC; Ser79), anti-phospho-AMPK (Thr172), anti-phospho-JNK (T183/Y185), anti-JNK, anti-phospho-p70S6K (Thr389), anti-cleaved caspase3, and anti-cleaved PARP antibodies were purchased from Cell Signaling (Danvers, MA). Anti-AMPK, anti-p70S6K, and anti-heat shock factor (HSF) antibodies were purchased from Santa Cruz Biotechnology (Santa Cruz, CA). Anti-phospho-HSF1 (Ser326), and anti-tubulin antibodies were from Abcam (Cambridge, UK). MG132, KRIBB 11, KNK-437, rapamycin, dorsomorphin, 17-AAG, bortezomib, metformin, and phenformin were purchased from Calbiochem (Sigma-Aldrich).

Real time-PCR. Real-time-PCR analyses were performed using ABI PRISM 7000 Sequence Detection System employing SYBR Green PCR Master Mix (Applied Biosystems, Foster City, CA), essentially as described (21, 24). The primers sets utilized in this study are summarized in Suppl. Table 1. Data are expressed as the mean level of expression normalized to actin, and represent the mean ± SEM of triplicate samples; results are representative of three independent experiments.

Cell proliferation, migration, invasion, and colony formation. Relative cell viability upon Hpa2 over-expression was assessed using MTT proliferation assay, essentially as described (25). Briefly, $2x10^3$ cells/well were seeded in 96 wells plate in medium supplemented with 2.5% FCS. At the indicated time points, 20 µl of MTT were added for 3 hours and absorbance at 570 nm was measured by a plate reader. Reduction of the MTT was calculated and presented as relative cell viability according to the manufacturer's (Bio-Rad; Hercules, CA) instructions. Migration and invasion assays were performed using modified Boyden chambers with polycarbonate Nucleopore membrane (6.5 mm in diameter, 8 µm pore-size; Corning, Corning, NY), coated with fibronectin (30 µl; 10 µg/ml; cell migration) or Matrigel (30 µl; cell invasion) essentially as described (26, 27). Colony formation in soft agar was performed as described (27). Briefly, Dulbecco's modified Eagle's medium (DMEM) (3 ml) containing 0.5% low-melt agarose (Bio-Rad) and 10% FCS was poured into 60-mm Petri dishes. The layer was covered with cell suspension ($2x10^3$ cells) in 1.5 ml DMEM containing 0.3% low-melt agarose and 10% FCS, followed by the addition of 2 ml DMEM containing 10% FCS. Medium was exchanged once a week. Colonies were visualized and counted under a microscope 2–5 weeks after seeding, as described (25, 28).

Cell lysates and protein blotting. Preparation of cell lysates and protein blotting were carried out essentially as described (24, 29).

Immunohistochemistry and immunofluorescent staining. Staining of formalin-fixed, paraffin-embedded 5-micron sections and immunofluorescent staining were performed essentially as described (30, 31). Specimens that were similarly stained with normal rabbit serum or by applying the above procedure but lacking the primary antibody yielded no detectable staining.

Tumorigenicity. Control (Vo) and Hpa2 overexpressing MGC-803 cells were detached with trypsin/EDTA, washed with PBS, and brought to a concentration of $5x10^6$ cells/ml. Cell suspension ($5x10^5$/0.1 ml) was inoculated intra-peritoneal to 6–10 week-old male NOD/SCID mice and the survival of mice was followed over time. All experiments were performed in accordance with the Technion's Institutional Animal Care and Use Committee (IL-080-08-2018; OPRR-A5026-01).

Statistics. Data are presented as means ± SE. Statistical significance was analyzed by 2-tailed Student's *t*-test. Values of $p < 0.05$ were considered significant. Data sets passed D'Agostino-Pearson normality (GraphPad Prism 5 utility software). All experiments were repeated at least 3 times with similar results.

Results

Clinical significance and pre-clinical studies. To reveal the clinical significance of Hpa2 in gastric cancer, we subjected tissue array of gastric carcinoma biopsies and adjacent normal gastric tissue to immunostaining applying anti-Hpa2 antibody. We found that 99% (78/79) of the normal gastric tissues were stained positive for Hpa2 (Fig. 1A, left panels) compared with 56% (54/96) of the gastric carcinomas (Table 1), differences that are statistically highly significant (p=0.0001). This implies that about half of the gastric carcinoma cases lose, or exhibit reduced Hpa2 expression (Fig. 1A, middle and right panels), an expression pattern typical of a tumor suppressor. Moreover, Hpa2 staining intensity correlated inversely with tumor stage (p=0.04; Table 2) and tumor metastasis to lymph nodes (N). Thus, most (54%) of the tumors that were stained strongly for Hpa2 had only a few infected lymph nodes (N1-N2), whereas patients with low levels of Hpa2 were mostly (67%) diagnosed with multiple infected lymph nodes (N3-N4), differences that are statistically highly significant (p=0.01; Table 2). Such a correlation between Hpa2 and tumor metastasis to lymph nodes was noted earlier in head and neck carcinoma (24). Notably, patients that exhibited high levels of Hpa2 (n=56, median survival time of 72 months) survived longer than patients with low Hpa2 levels (n=79, median survival time of 23 months) (Fig. 1B; p=0.004). This suggests that in gastric cancer, Hpa2 functions to restrain tumor growth.

To further explore the role of Hpa2 in gastric cancer we next transfected gastric carcinoma cell lines with Hpa2 gene construct and examined their tumorigenic capacities in vitro. We found that proliferation of MKN-45 cells was attenuated markedly following Hpa2 overexpression (Fig. 2A; p<0.0001). Likewise, migration of MKN-45-Hpa2 cells was prominently reduced compared with control (Vo) cells (Fig. 2B; p<0.0001). Furthermore, the capacity of MKN-45 (Fig. 2C, upper panel), SGC-7901 (Fig. 2C, middle panels), and BGC-823 (Fig. 2C, lower panels) to form colonies in soft agar was attenuated following Hpa2 overexpression compared with control (Vo) cells. We next implanted control (Vo) and Hpa2 overexpressing MGC-803 cells intra-peritoneal (ip) and the survival time of the mice was followed. This model is most relevant because peritoneal metastases occur in 55-60% of patients with gastric cancer, associating with a low (2%) 5-year overall survival rate (3). Notably, mice implanted with Hpa2 cells survived significantly longer than control (Fig. 2D; p=0.0003). In a subsequent experiment, mice were similarly implanted with control (Vo) and Hpa2 cells, sacrificed 14 days later, and tumor lesions were collected. Remarkably, mice implanted with Hpa2 cells exhibited reduced tumor mass collected from the

peritoneum (Fig. 2E), also evident by reduced amounts of ascites fluids collected (Suppl. Fig. 1A). Collectively, these results suggest that Hpa2 attenuates the tumorigenic properties of gastric carcinoma cells.

Hpa2 expression is induced by stress, involving HSF1 and AMPK. Reduced Hpa2 expression in some of the gastric carcinomas and its high expression in others (Fig. 1A) suggests that Hpa2 expression is tightly regulated. However, mechanisms that regulate Hpa2 gene expression have not been explored yet. We hypothesized that conditions of stress, which are often associated with the fast-growing tumor and the dynamic nature of the tumor microenvironment, are involved in Hpa2 gene regulation. To examine this possibility, we exposed gastric carcinoma cell lines to MG132, an inhibitor of the proteasome, which results in severe proteotoxic stress (32). Consistently, we found that Hpa2 expression was induced 10-30 folds by the proteotoxic stress elicited by MG132 in MKN-45, BGC-823, AGS, and MGC cells in a time-, and dose-dependent manner (Fig. 3A-D). Moreover, Hpa2 expression was induced to a comparable extent by bortezomib (Velcade) (Fig. 3E, F), a proteasome inhibitor that is most effective in the treatment of multiple myeloma patients and is also effective in gastric cancer (33). Hpa2 gene induction was similarly observed in non-transformed cells such as mouse embryonic fibroblasts (MEF, Suppl. Fig. 1B, upper panel), and in mouse Lewis lung carcinoma cells (Suppl. Fig. 1C, upper panel). In these cells, as well as in gastric carcinoma cells, the stress conditions also induced the expression of cytokines such as MIP2 (Suppl. Fig. 1B, C middle panels) and TNF-α (Suppl. Fig. 1B, C lower panels) that have a profound impact on the immune system and the tumor microenvironment.

To examine the molecular mechanism underlying Hpa2 induction, we subjected gastric carcinoma cells to MG132 for increasing periods and protein extracts were subjected to immunoblotting. Consistently, we found that MG132 treatment resulted in a profound increase in the phosphorylation levels of AMPK (Fig. 4A, upper panels), JNK (Fig. 4A, fifth panels), and p70S6K (pS6K; Fig. 4A, seventh panels), the latter is indicative of mTOR activation. We also found that MG132 enhances the phosphorylation of heat shock factor-1 (HSF1; Fig. 4A, third panels), while HSF1 expression was not affected (Fig. 4A, fourth panels). Notably, the increased phosphorylation of HSF1 was associated with a profound increase in the expression levels of heat shock protein (HSP) 40, 105, 27, and 70 (Suppl. Fig. 2A), a consequence of HSF1 activation because this increase in HSP expression was abrogated by HSF1 inhibitors KRIBB 11 and KNK-437 (Suppl. Fig. 2B). To tie between Hpa2 induction and the signaling pathways elicited by the stress, we treated MKN-45 cells with MG132 in the absence or presence of inhibitors specific for each signaling pathway. We found that Hpa2 induction by MG132 was attenuated markedly by KRIBB 11, an inhibitor of HSF1, and by dorsomorphin (Dor), an inhibitor of AMPK (Fig. 4B, red arrows; Fig. 4C, upper and middle panels). In contrast, Hpa2 gene induction by MG132 was not affected by rapamycin (inhibitor of mTOR) (Fig. 4B) or sp600125 (a JNK inhibitor), thus pointing to AMPK and HSF1 as modulators of Hpa2 expression. Moreover, silencing of HSF and AMPK-beta resulted in reduced Hpa2 expression (Fig. 4C, lower panel), further supporting the significance of these pathways in Hpa2 gene regulation. Notably, subjecting control (Vo) and Hpa2 overexpressing MKN-45 cells to MG132 revealed increased levels of cleaved caspase 3 and cleaved PARP in Hpa2 cells vs control (Vo) cells (Fig. 4D), suggesting that Hpa2 cells are more sensitive to proteotoxic stress conditions, resulting in increased apoptosis.

Hpa2 enhances AMPK phosphorylation. We next attempted to reveal signaling pathways that are modulated by Hpa2 and may be responsible for the observed reduced tumorigenic properties (Figs. 1, 2) and higher sensitivity to conditions of stress (Fig. 4D). Immunoblot analyses of cell extracts derived from control and Hpa2 overexpressing MKN-45 (Fig. 5A, left panels), BGC823 (Fig. 5A, middle panels) and SGC7901 (Fig. 5A, right panels) cells revealed a consistent increase in the phosphorylation of AMPK (Fig. 5A, upper panels) and its substrate, acetyl CoA carboxylase (pACC; Fig. 5A, third panels). Increased ACC phosphorylation by Hpa2 was also evident by immunofluorescent staining (Fig. 5B). Moreover, we found that the increase in ACC phosphorylation in Hpa2 cells was reversed by adding heparin to the cell culture medium (Fig. 5C), suggesting that this effect involves the interaction of Hpa2 with cell membrane HS (20). Enhanced phosphorylation of AMPK is relevant to the anti-tumorigenic properties of Hpa2 because AMPK activation is found in correlation with good prognosis of cancer patients, including gastric cancer patients (1, 34). Also, we found reduced phosphorylation of HSF1 in Hpa2 cells (pHSF1; Fig. 5A, fifth panels, BGC, SGS). This finding is important because HSF1 exerts a pro-tumorigenic effect in many types of cancer, including gastric cancer (35, 36). In order to study the significance of AMPK in gastric carcinoma, we applied metformin, a drug that induces the phosphorylation of AMPK (Suppl. Fig. 3A) and is used in the clinic to treat diabetic patients (37, 38). Notably, the proliferation of MKN-45 cells was attenuated markedly by metformin in a dose-dependent manner (Suppl. Fig. 3B) while inducing the expression of Hpa2 (Suppl. Fig. 3C). Furthermore, we found that metformin treatment reduced the invasion (Fig. 6A), migration (Fig. 6B, C), and colony formation by gastric carcinoma cells to an extent comparable to Hpa2 (Fig. 6A-D, Vo+Met vs Hpa2). These results suggest that the anti-tumorigenic properties of Hpa2 in gastric carcinoma are mediated, at least in part, by enhancing the phosphorylation of AMPK.

Given that Hpa2 is highly expressed in normal gastric tissue (Fig. 1A, left), we next examined the correlation between Hpa2 levels and AMPK phosphorylation in this tissue. We found that AMPK is phosphorylated in about half of the gastric tissues examined (43/93; Table 3) and, like Hpa2, is decreased prominently in gastric cancer (Fig. 5D; N=normal, T=Tumor). Importantly, gastric tissues that exhibit high levels of AMPK phosphorylation (Fig. 5D, E) are also stained positive for Hpa2 (Table 3; $p=0.02$). These results imply that Hpa2 functions to modulate AMPK phosphorylation and metabolic aspects in normal gastric epithelial cells.

Discussion

Hpa2 was cloned shortly after the cloning of heparanase (18) but acquired very little attention, possibly because it lacks HS-degrading activity typical of heparanase (20). The emerging role of Hpa2 in a rare autosomal recessive congenital disease called urofacial syndrome (UFS) (39–41) indicates that Hpa2 plays an important role in human disorders. In UFS, biallelic mutations of Hpa2 mostly result in frame-shifts that lead to an early stop codon and a truncated Hpa2 protein, resulting in a loss-of-function phenotype (39, 40). The lack of Hpa2 appears to be responsible for peripheral neuropathy of the bladder, typical of UFS (42, 43) and likely affects facial nerves because people with UFS have a characteristic grimace upon smiling, indicating that Hpa2 plays a critical role in neuronal function.

The role of Hpa2 in normal epithelial cells has not been investigated yet. Here, we found that increased AMPK phosphorylation in human gastric epithelial cells correlates with high levels of Hpa2 (Table 3), suggesting that Hpa2 functions to modulate AMPK phosphorylation in normal epithelia. This feature is of high importance, given the immense role of AMPK in energy sensing and cell metabolism (44, 45), thus implying that Hpa2 regulates metabolic processes. Maintaining high levels of AMPK phosphorylation in normal epithelia is also important for tumorigenesis because AMPK was reported to protect normal epithelia from oncogenic transformation (46). It is yet to be demonstrated whether changes in AMPK activity are also relevant to UFS and the neuropathies associated with Hpa2-deficient neurons (43).

Given the tumor-suppressive properties of AMPK (46–48), increased AMPK phosphorylation by human gastric carcinoma cells overexpressing Hpa2 (Fig. 5) supports the notion that Hpa2 functions to attenuate tumor growth. This notion is reinforced by the following observations. Hpa2 expression was noted to be substantially decreased in breast, ovarian, bladder (19, 49, 50) and gastric (Fig. 1; Table 1) carcinomas vs adjacent normal tissues, expression pattern typical of tumor suppressors. Notably, bladder (51) tumors that retain high levels of Hpa2 are diagnosed as low grade, indicating that Hpa2 likely functions to maintain epithelial cell differentiation. In head and neck cancer, patients scored to express high levels of Hpa2 survive longer than patients exhibiting low levels of Hpa2 (20). Prolonged survival is now also shown here for gastric cancer patients exhibiting high levels of Hpa2 (Fig. 1), together suggesting that Hpa2 functions to suppress tumorigenesis. The cellular and molecular mechanism(s) exerted by Hpa2 to attenuate tumorigenicity are largely obscure. Previously, we have reported that head and neck cancer patients expressing high levels of Hpa2 show reduced lymph node metastasis (20), and overexpression of Hpa2 in FaDu pharyngeal carcinoma cells resulted in smaller tumors that exhibited a marked decrease in tumor vascularity (blood and lymph vessels) (24). Our results suggest an additional molecular mechanism exerted by Hpa2 to restrain tumor growth. Namely, we report here for the first time that Hpa2 enhances the phosphorylation of AMPK and its activity, reflected by increased phosphorylation of its substrate, ACC, in gastric (Fig. 5A, B) and pharyngeal (Suppl. Figure 3D) carcinoma cells. This finding is both important and relevant because cancer patients, including gastric cancer patients, with high levels of AMPK phosphorylation, are endowed with good prognosis (1). The anti-tumorigenic properties of AMPK are best exemplified by an intense effort to develop compounds that activate AMPK as anti-cancer medications (47). A prototype of such AMPK activators is metformin (37) that is evaluated as anti-cancer drug for many types of cancer (47). Notably, metformin attenuated cell proliferation, migration, invasion, and colony formation by gastric carcinoma cells to an extent comparable with Hpa2 (Fig. 6, Suppl. Figure 3), suggesting that these properties of Hpa2 are mediated, at least in part, by AMPK.

We also found that overexpression of Hpa2 in gastric carcinoma cells results in decreased phosphorylation of HSF1 (Fig. 5). This is important and relevant to the tumor suppressor properties of Hpa2 because HSF1 is found pro-tumorigenic in various types of cancer including gastric cancer, and is a target for the development of anti-cancer therapeutics (35, 52). Notably, increased AMPK phosphorylation and decreased HSF1 phosphorylation may be related because AMPK was found to physically interacts with HSF1 and to phosphorylates it at Ser121, a residue that suppresses HSF1 activity (52). Thus, Hpa2

appears to enhance anti-tumorigenic (AMPK phosphorylation) and decrease pro-tumorigenic (HSF1) pathways, leading to decreased tumor burden (Fig. 2) and prolonged survival of gastric patients (Fig. 1).

Substantial changes in Hpa2 staining intensities between normal and tumor lesions (Fig. 1) (19, 49, 50, 53) strongly suggest that Hpa2 expression is tightly regulated, but mechanisms that regulate Hpa2 expression have not been elucidated yet. Here, we report for the first time that Hpa2 expression is prominently induced by conditions of stress. Notably, treatment of normal (MEF) and tumor-derived cells with MG132, an inhibitor of the proteasome that results in proteotoxic stress, prominently enhances Hpa2 expression (Fig. 3, Suppl. Figure 1). Interestingly, Hpa2 induction by MG132 appeared to be mediated by AMPK and HSF1 because specific inhibitors of AMPK (dorsomorphin) and HSF1 (KRIBB 11) prevented Hpa2 induction by MG132 (Fig. 4). These results imply the occurrence of a cycle that feeds itself, by which Hpa2 enhances AMPK phosphorylation that, in turn, induces Hpa2 expression.

Conclusions

These results indicate that high levels of Hpa2 in some tumors but not in others are due to stress conditions that tumors often experience due to their high rates of cell proliferating, high metabolic demands, and changes in the tumor microenvironment. This increase in Hpa2 levels by the stressed tumors appears critically important for the patient's outcome.

Abbreviations

ACC- Acetyl CoA carboxylase

AMPK- AMP-activated protein kinase

ECM- Extracellular matrix

HSPG- Heparan sulfate proteoglycans

HS- Heparan Sulfate

HSF- Heat shock factor

HSP- Heat shock protein

MEF- Mouse embryonic fibroblasts

UFS- Urofacial syndrome

Declarations

Ethics approval and consent to participate: Human data. Approval is waived given that we have used commercial tissue arrays purchased from Outdo Biotech Co., Ltd. (http://www.superchip.com.cn/) and

from US Biomax (Rockville, MD) as detailed under 'Materials & Methods'. Samples are not collected by interacting or intervening with living people. None of the investigators or collaborators can identify the subjects through coded private information or specimens (NIH exemption #4). Helsinki approval for the use of human tissues (0667-19-RMC) was issued on 21/11/2019 by Rambam Health Care Campus, Helsinki Committee. Animals. All experiments were performed in accordance with the Technion's Institutional Animal Care and Use Committee (IL-080-08-2018; OPRR-A5026-01). See 'Materials & Methods'.

Consent for publication. Not applicable

Availability of data and materials. The datasets obtained and/or analyzed during the current study are available from the corresponding author on reasonable request. All data generated or analyzed during this study are included in this published article [and its supplementary information files].

Competing interests. The authors declare that they have no competing interests.

Funding: These studies were generously supported by research grants awarded by the Israel Science Foundation (ISF grant 1021/19), the NSFC-ISF cooperation program (grant 2572/16) between the National Natural Science Foundation of China (NSFC) and the Israel Science Foundation (ISF), and the Israel Cancer Research Fund (ICRF). I. Vlodavsky is a Research Professor of the ICRF.

Author contribution :IV, NI, SY Concepted and designed the work; JL, IK, MG-C, HJ, WS, TL, NI performed, acquisited, analyzed, or interpretated the data; NI, IV, SY drafted the work or substantively revised it. All authors read and approved the final manuscript.

Acknowledgments. Not applicable

References

1. Kim JG, Lee SJ, Chae YS, Kang BW, Lee YJ, Oh SY, et al. Association between phosphorylated AMP-activated protein kinase and MAPK3/1 expression and prognosis for patients with gastric cancer. Oncology. 2013;85:78-85.
2. Bray F, Ferlay J, Soerjomataram I, Siegel RL, Torre LA, Jemal A. Global cancer statistics 2018: GLOBOCAN estimates of incidence and mortality worldwide for 36 cancers in 185 countries. CA Cancer J Clin. 2018;68:394-424.
3. Yao X, Ajani JA, Song S. Molecular biology and immunology of gastric cancer peritoneal metastasis. Transl Gastroenterol Hepatol. 2020;5:57.
4. Bernfield M, Gotte M, Park PW, Reizes O, Fitzgerald ML, Lincecum J, et al. Functions of cell surface heparan sulfate proteoglycans. Ann Rev Biochem. 1999;68:729-77.
5. Iozzo RV, Sanderson RD. Proteoglycans in cancer biology, tumour microenvironment and angiogenesis. J Cell Mol Med. 2011;15:1013-31.

6. Karamanos NK, Piperigkou Z, Theocharis AD, Watanabe H, Franchi M, Baud S, et al. Proteoglycan chemical diversity drives multifunctional cell regulation and therapeutics. Chem Rev. 2018;118:9152-232.
7. Coombe DR, Gandhi NS. Heparanase: A challenging cancer drug target. Front Oncol. 2019;9:1316.
8. Khanna M, Parish CR. Heparanase: Historical aspects and future perspectives. Adv Exp Med Biol. 2020;1221:71-96.
9. Vlodavsky I, Ilan N, Sanderson RD. Forty years of basic and translational heparanase research. Adv Exp Med Biol. 2020;1221:3-59.
10. Billings PC, Pacifici M. Interactions of signaling proteins, growth factors and other proteins with heparan sulfate: mechanisms and mysteries. Connect Tissue Res. 2015;56:272-80.
11. Rivara S, Milazzo FM, Giannini G. Heparanase: a rainbow pharmacological target associated to multiple pathologies including rare diseases. Future Med Chem. 2016;8:647-80.
12. Vlodavsky I, Singh P, Boyango I, Gutter-Kapon L, Elkin M, Sanderson RD, et al. Heparanase: From basic research to therapeutic applications in cancer and inflammation. Drug Res Updates. 2016;29:54-75.
13. Dredge K, Brennan TV, Hammond E, Lickliter JD, Lin L, Bampton D, et al. A Phase I study of the novel immunomodulatory agent PG545 (pixatimod) in subjects with advanced solid tumours. Br J Cancer. 2018;118:1035-41.
14. Galli M, Chatterjee M, Grasso M, Specchia G, Magen H, Einsele H, et al. Phase I study of the heparanase inhibitor roneparstat: an innovative approach for ultiple myeloma therapy. Haematologica. 2018;103:e469-e72.
15. Tang B, Yang S. Involvement of heparanase in gastric cancer progression and immunotherapy. Adv Exp Med Biol. 2020;1221:351-63.
16. Li HL, Gu J, Wu JJ, Ma CL, Yang YL, Wang HP, et al. Heparanase mRNA and protein expression correlates with clinicopathologic features of gastric cancer patients: a Meta- analysis. Asian Pac J Cancer Prev. 2015;16:8653-8.
17. Takaoka M, Naomoto Y, Ohkawa T, Uetsuka H, Shirakawa Y, Uno F, et al. Heparanase expression correlates with invasion and poor prognosis in gastric cancers. Lab Invest. 2003;83:613-22.
18. McKenzie E, Tyson K, Stamps A, Smith P, Turner P, Barry R, et al. Cloning and expression profiling of Hpa2, a novel mammalian heparanase family member. Biochem Biophys Res Commun. 2000;276:1170-7.
19. Vlodavsky I, Gross-Cohen M, Weissmann M, Ilan N, Sanderson RD. Opposing Functions of Heparanase-1 and hHeparanase-2 in cancer progression. Trends Biochem Sci. 2018;43:18-31.
20. Levy-Adam F, Feld S, Cohen-Kaplan V, Shteingauz A, Gross M, Arvatz G, et al. Heparanase 2 interacts with heparan sulfate with high affinity and inhibits heparanase activity. J Biol Chem. 2010;285:28010-9.

21. Gutter-Kapon L, Alishekevitz D, Shaked Y, Li JP, Aronheim A, Ilan N, et al. Heparanase is required for activation and function of macrophages. Proc Natl Acad Sci USA. 2016;113:E7808-E17.
22. Hao NB, Tang B, Wang GZ, Xie R, Hu CJ, Wang SM, et al. Hepatocyte growth factor (HGF) upregulates heparanase expression via the PI3K/Akt/NF-kappaB signaling pathway for gastric cancer metastasis. Cancer Lett. 2015;361:57-66.
23. Tang B, Xie R, Qin Y, Xiao YF, Yong X, Zheng L, et al. Human telomerase reverse transcriptase (hTERT) promotes gastric cancer invasion through cooperating with c-Myc to upregulate heparanase expression. Oncotarget. 2016;7:11364-79.
24. Gross-Cohen M, Feld S, Doweck I, Neufeld G, Hasson P, Arvatz G, et al. Heparanase 2 attenuates head and neck tumor vascularity and growth. Cancer Res. 2016;76:2791-801.
25. Barash U, Spyrou A, Liu P, Vlodavsky E, Zhu C, Luo J, et al. Heparanase promotes glioma progression via enhancing CD24 expression. Intl J Cancer. 2019;145:1596-608.
26. Arvatz G, Barash U, Nativ O, Ilan N, Vlodavsky I. Post-transcriptional regulation of heparanase gene expression by a 3' AU-rich element. Faseb J. 2011;24:4969-76.
27. Barash U, Zohar Y, Wildbaum G, Beider K, Nagler A, Karin N, et al. Heparanase enhances myeloma progression via CXCL10 downregulation. Leukemia. 2014;28:2178-87.
28. Barash U, Lapidot M, Zohar Y, Loomis C, Moreira A, Feld S, et al. Involvement of heparanase in the pathogenesis of mesothelioma: Basic aspects and clinical applications. J Natl Cancer Inst. 2018;110:1102-14.
29. Bhattacharya U, Gutter-Kapon L, Kan T, Boyango I, Barash U, Yang SM, et al. Heparanase and chemotherapy synergize to drive macrophage activation and enhance tumor growth. Cancer Res. 2020;80:57-68.
30. Shteingauz A, Ilan N, Vlodavsky I. Processing of heparanase is mediated by syndecan-1 cytoplasmic domain and involves syntenin and alpha-actinin. Cell Mol Life Sci. 2014;71:4457-70.
31. Weissmann M, Arvatz G, Horowitz N, Feld S, Naroditsky I, Zhang Y, et al. Heparanase-neutralizing antibodies attenuate lymphoma tumor growth and metastasis. Proc Natl Acad Sci USA. 2016;113:704-9.
32. Lee DH, Goldberg AL. Proteasome inhibitors: valuable new tools for cell biologists. Trends Cell Biology. 1998;8:397-403.
33. Nakata W, Hayakawa Y, Nakagawa H, Sakamoto K, Kinoshita H, Takahashi R, et al. Anti-tumor activity of the proteasome inhibitor bortezomib in gastric cancer. Int J Oncol. 2011;39:1529-36.
34. Kuhajda FP. AMP-activated protein kinase and human cancer: cancer metabolism revisited. Int J Obes (Lond). 2008;32 Suppl 4:S36-41.
35. Dai W, Ye J, Zhang Z, Yang L, Ren H, Wu H, et al. Increased expression of heat shock factor 1 (HSF1) is associated with poor survival in gastric cancer patients. Diagn Pathol. 2018;13:80.
36. Saini J, Sharma PK. Clinical, Prognostic and Therapeutic significance of heat shock proteins in cancer. Curr Drug Targets. 2018;19:1478-90.

37. Piskovatska V, Storey KB, Vaiserman AM, Lushchak O. The use of metformin to increase the human healthspan. Adv Exp Med Biol. 2020;1260:319-32.
38. Aljofan M, Riethmacher D. Anticancer activity of metformin: a systematic review of the literature. Future Sci OA. 2019;5:FSO410.
39. Daly SB, Urquhart JE, Hilton E, McKenzie EA, Kammerer RA, Lewis M, et al. Mutations in HPSE2 cause urofacial syndrome. Am J Hum Genet. 2010;86:963-9.
40. Pang J, Zhang S, Yang P, Hawkins-Lee B, Zhong J, Zhang Y, et al. Loss-of-function mutations in HPSE2 cause the autosomal recessive urofacial syndrome. Am J Hum Genet. 2010;86:957-62.
41. Stuart HM, Roberts NA, Hilton EN, McKenzie EA, Daly SB, Hadfield KD, et al. Urinary tract effects of HPSE2 mutations. J Am Soc Nephrol. 2015;26:797-804.
42. Roberts NA, Hilton EN, Lopes FM, Singh S, Randles MJ, Gardiner NJ, et al. Lrig2 and Hpse2, mutated in urofacial syndrome, pattern nerves in the urinary bladder. Kidney Intl. 2019;95:1138-52.
43. Roberts NA, Woolf AS. Heparanase 2 and Urofacial Syndrome, a Genetic Neuropathy. Adv Exp Med Biol. 2020;1221:807-19.
44. Hardie DG, Schaffer BE, Brunet A. AMPK: An energy-sensing pathway with multiple inputs and outputs. Trends Cell Biol. 2016;26:190-201.
45. Ross FA, MacKintosh C, Hardie DG. AMP-activated protein kinase: a cellular energy sensor that comes in 12 flavours. The FEBS J. 2016;283:2987-3001.
46. Vara-Ciruelos D, Russell FM, Hardie DG. The strange case of AMPK and cancer: Dr Jekyll or Mr Hyde? (dagger). Open Biol. 2019;9:190099.
47. Steinberg GR, Carling D. AMP-activated protein kinase: the current landscape for drug development. Nat Rev Drug Discov. 2019;18:527-51.
48. Zhang J, Wen L, Zhou Q, He K, Teng L. Preventative and therapeutic effects of metformin in gastric cancer: A new contribution of an old friend. Cancer Manag Res. 2020;12:8545-54.
49. Fu J, Khaybullin R, Zhang Y, Xia A, Qi X. Gene expression profiling leads to discovery of correlation of matrix metalloproteinase 11 and heparanase 2 in breast cancer progression. BMC Cancer. 2015;15:473.
50. Ilan N, Bhattacharya U, Barash U, Boyango I, Yanku Y, Gross-Cohen M, et al. Heparanase-The message comes in different flavors. Adv Exp Med Biol. 2020;1221:253-283.
51. Gross-Cohen M, Feld S, Naroditsky I, Nativ O, Ilan N, Vlodavsky I. Heparanase 2 expression inversely correlates with bladder carcinoma grade and stage. Oncotarget. 2016;7:22556-65.
52. Kijima T, Prince T, Neckers L, Koga F, Fujii Y. Heat shock factor 1 (HSF1)-targeted anticancer therapeutics: overview of current preclinical progress. Expert Opin Ther Targets. 2019;23:369-77.
53. Doweck I, Feibish N. Opposing effects of heparanase and heparanase-2 in head & neck cancer. Adv Exp Med Biol. 2020;1221:847-56.

Tables

Table 1. Hpa2 levels are decreased in gastric carcinoma vs normal gastric tissue

	Hpa2		
	Negative	Positive	Total
Normal	1 (1)	78 (**99**)	79
Malignant	42 (44)	54 (56)	96
p<0.0001	43	132	175

Table 2. Pathological characterization of the gastric carcinoma patients in correlation with Hpa2 staining intensity.

		HPA2			
	Total	**Low (%)**	**High (%)**	**χ2 value**	**p value**
Gender					
male	101	57 (56)	44 (44)		
female	33	21 (63)	12 (37)	0.53	0.4
Age					
<65	62	27 (43)	35 (57)		
≥65	73	52 (71)	21 (29)	10.585	**0.001**
Volume					
<5cm	54	24 (44)	30 (56)		
≥5cm	77	52 (67)	25 (33)	6.946	0.008
T					
T1-T2	26	12 (46)	14 (54)		
T3-T4	95	57 (60)	38 (40)	1.597	0.2
N					
N1-N2	58	27 (46)	31 (54)		
N3-N4	76	51 (67)	25 (33)	5.713	**0.01**
M					
M0	128	74 (57)	54 (43)		
M1	7	5 (71)	2 (29)	0.507	0.4
Stage					
□-□	54	26 (48)	28 (52)		
□-□	73	48 (65)	25 (35)	3.956	**0.04**

Table 3. Hpa2 levels correlates with AMPK phosphorylation in normal gastric tissue

Hpa2 / pAMPK	Negative (%)	Positive (%)	Total
Negative	6 (12)	44 (88)	50
Positive	0 (0)	43 (100)	43
p=0.02	6	87	93

Figures

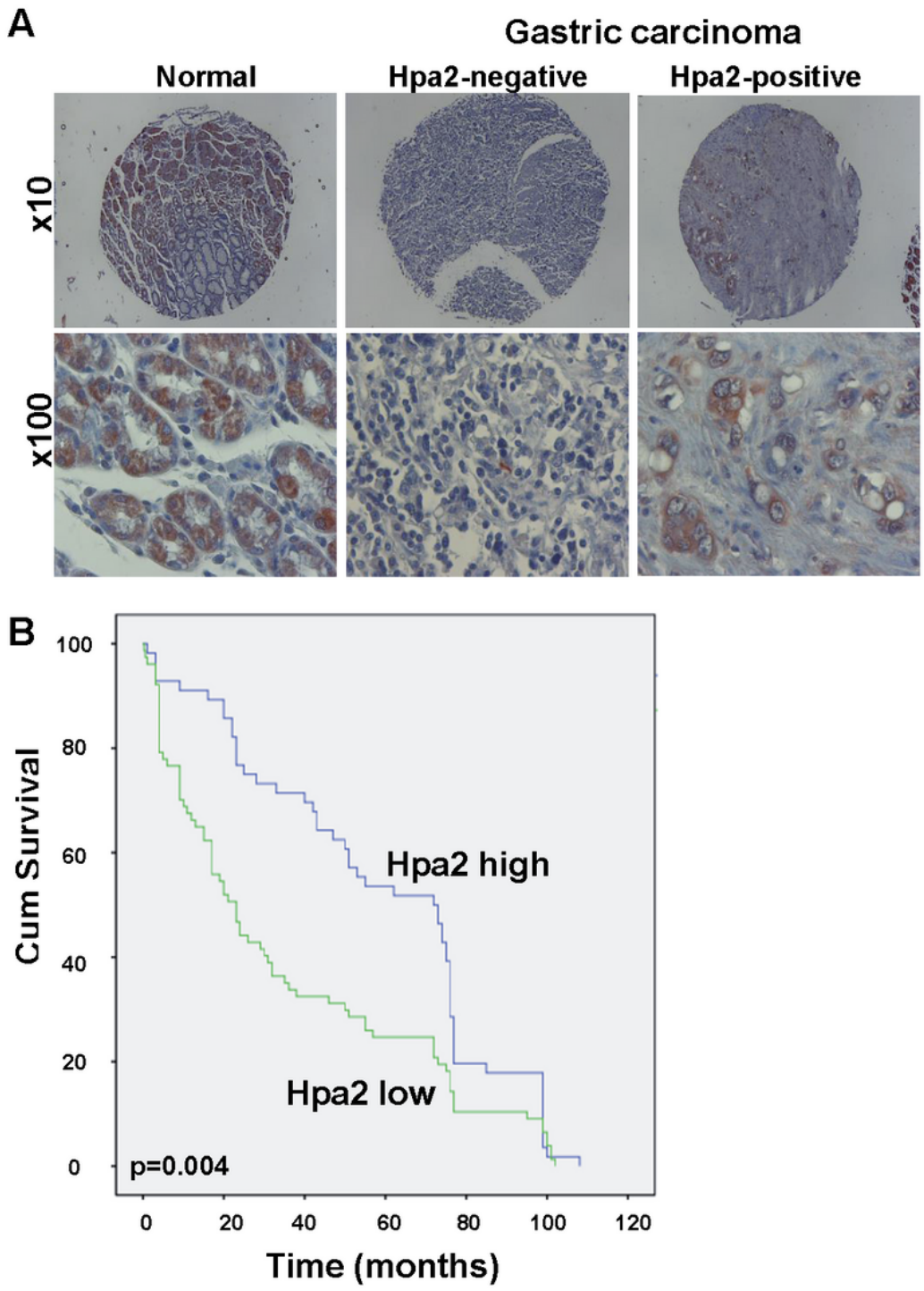

Figure 1

High levels of Hpa2 are associated with longer survival of gastric cancer patients. A. Immunostaining. Tumor biopsies and adjacent normal gastric tissues were subjected to immunostaining applying anti-Hpa2 antibody. Shown are representative images of Hpa2 staining in normal gastric tissue (left) and gastric carcinoma stained negative (middle) and positive (right) for Hpa2. Original magnifications: x10 (upper panels), x100 (lower panels). B. Kaplan-Meier survival plot. Kaplan-Meier survival analysis of

gastric cancer patients according to their Hpa2 staining intensities (high vs low). Gastric carcinoma patients exhibiting strong staining of Hpa2 (n=56) survive significantly longer than patients that show low levels of Hpa2 (n=79; p=0.004).

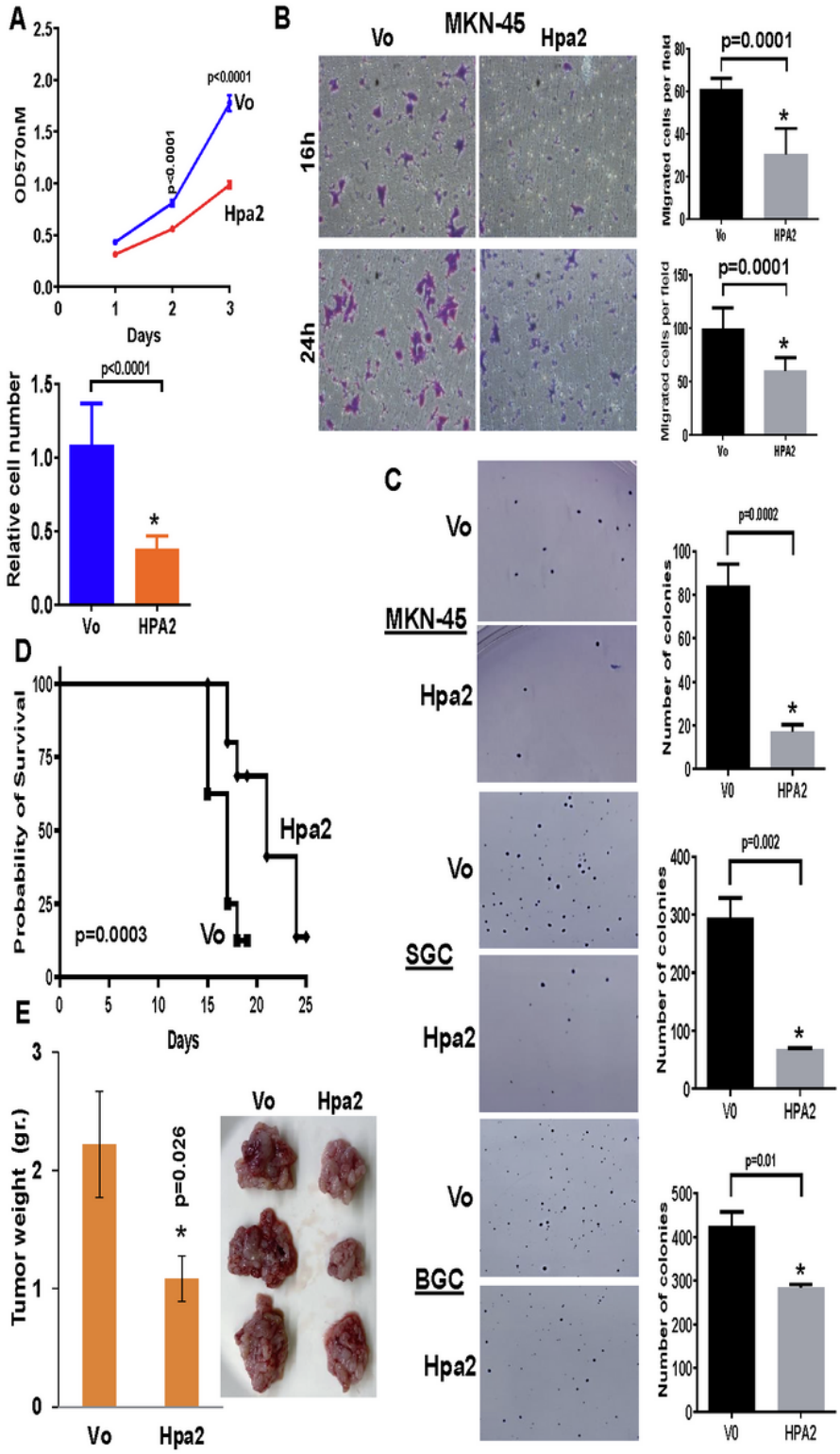

Figure 2

Overexpression of Hpa2 attenuates the pro-tumorigenic characteristics of gastric carcinoma cells. A. Cell proliferation. Control (Vo) and Hpa2 overexpressing MKN-45 cells (2x103/well) were seeded in a 96-well

plate and relative cell numbers were examined over time as described under 'Materials and methods' (upper panel). The relative number of Hpa2 cells at day 3 is shown graphically vs control (Vo) cells set arbitrarily to a value of 1 (lower panel). B. Cell migration. Control (Vo) and Hpa2 overexpressing MKN-45 cells were seeded on fibronectin-coated inserts and cell migration was examined 16 hours (upper panels) and 24 hours (lower panels) afterword. Shown are representative images taken at x20 magnification. The number of migrating cells is shown graphically in the right panels. C. Colony formation. Control (Vo) and Hpa2 overexpressing MKN-45 (upper panels), SGC-7901 (middle panels), and BGC-832 (lower panels) cells were grown in soft agar as described under 'Materials and methods'. After 3-4 weeks, dishes were fixed with formalin and cell colonies were stained with Crystal violet. Representative photomicrographs are shown in the left panels (original magnifications x10). Quantification of the number of colonies per dish is shown graphically in the right panels. D, E. Survival times and tumor growth. Control (Vo) and Hpa2 overexpressing MGC-803 cells (0.5x106) were injected intraperitoneal (ip) into NOD/SCID mice (n=7) and survival times recorded (D). Control and Hpa2 MGC-803 cells were similarly inoculated ip into NOD/SCID mice (n=7). After 14 days mice were sacrificed and all the tumor lesions from each mouse were collected, weighed (E, left) and photographed. Shown are representative images of the tumor lesions collected from mice implanted with control (Vo) and Hpa2 cells (E, right).

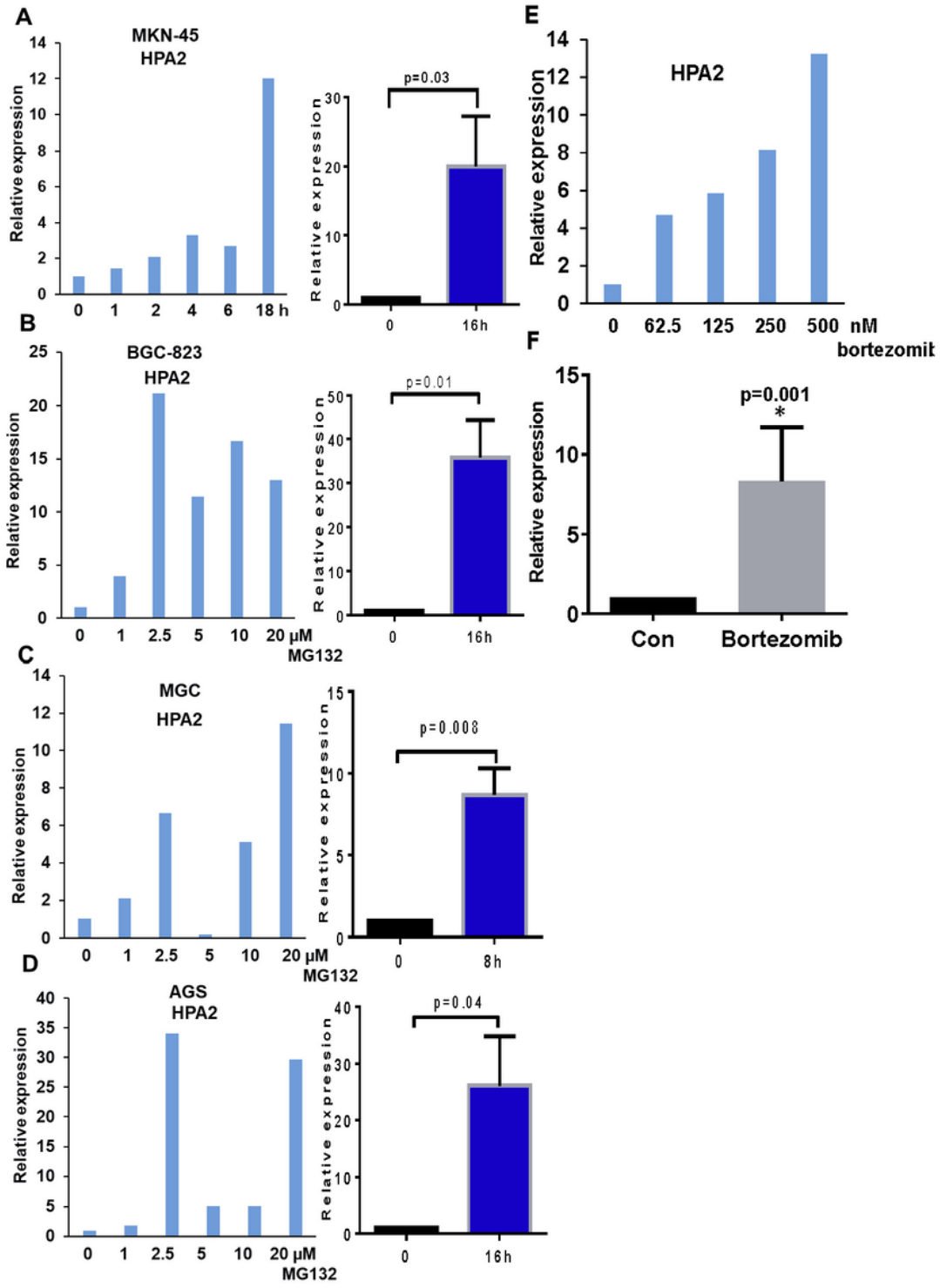

Figure 3

Hpa2 expression is induced by MG132. A-D. The indicated gastric carcinoma cell lines were treated with the indicated concentrations of MG132, or with MG132 (20 µM) for the indicated time. Control cells (0) were treated with vehicle (DMSO). Total RNA was then extracted and subjected to qPCR applying primers specific for Hpa2. Hpa2 expression (fold increase) in response to MG132 treatment for 16 hours is shown graphically in the right panels vs control untreated cells (0), set arbitrarily to a value of 1, and after

normalization to actin. E. Bortezomib treatment. MKN-45 cells were treated with the indicated concentration of bortezomib for 16 hours and Hpa2 expression was quantified by qPCR (upper panel). Average Hpa2 expression (fold-increase) by bortezomib treated cells vs control (0) is shown graphically (lower panel).

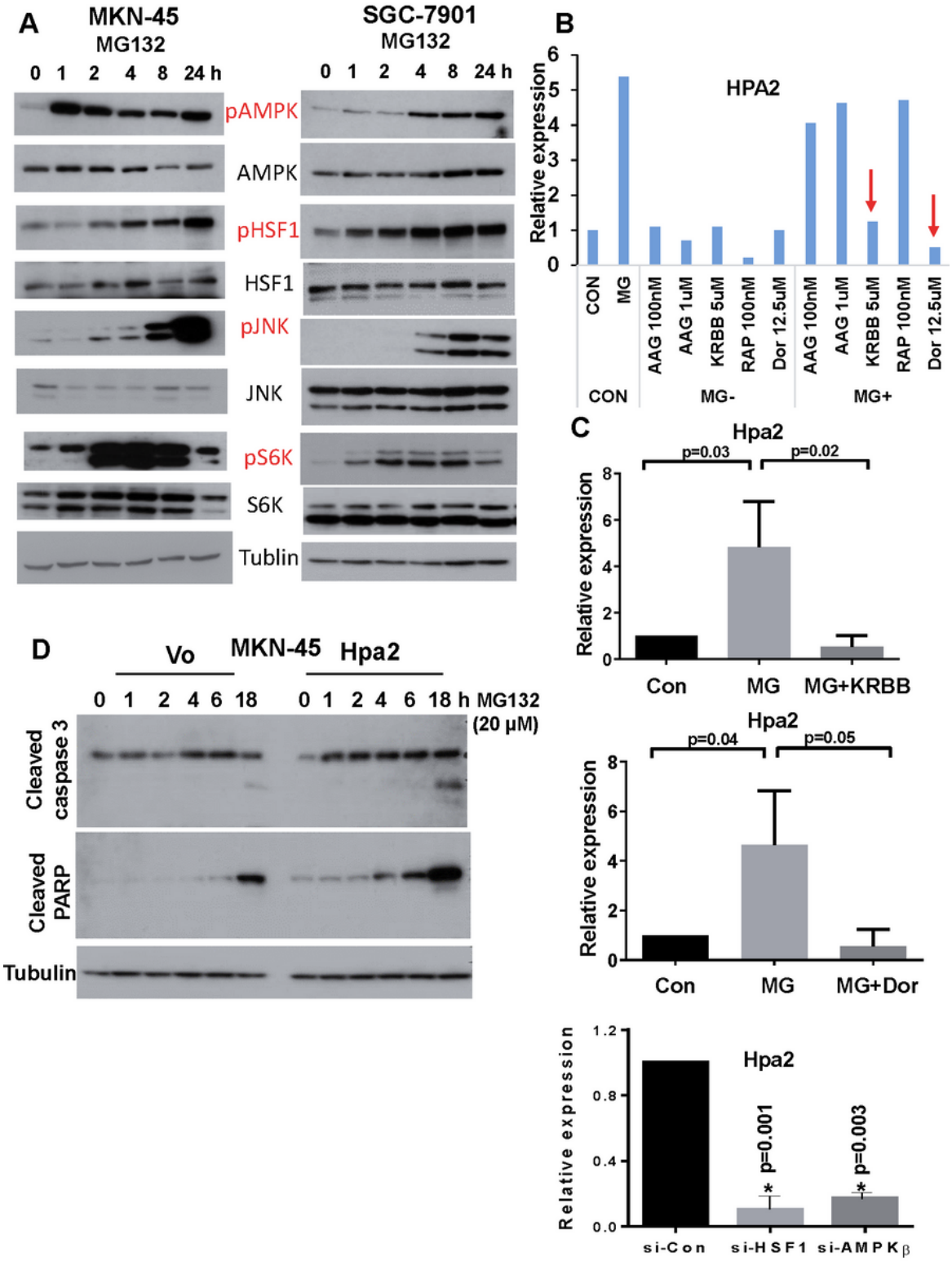

Figure 4

Hpa2 induction by MG132 involves AMPK and HSF1. A. Immunoblotting. MKN-45 (left) and SFC-7901 (right) gastric carcinoma cells were left untreated (0) or were treated with MG132 (20 μM) for the time indicated. Cell extracts were then prepared and subjected to immunoblotting applying antibodies directed to phospho-AMPK (pAMPK; upper panels), AMPK (second panels), phospho-HSF1 (pHSF1; third panels), HSF1 (fourth panels), phospho-JNK (fifth panels), JNK (sixth panels), phospho-p70S6K (pS6K; seventh panels), S6K (eight panels), and tubulin (lower panels). B. Inhibitors. MKN-45 cells were similarly treated with vehicle (DMSO; Con) or MG132 without (MG) or with the indicated concentrations of 17-AAG (AAG) (HSP90 inhibitor), KRIBB 11 (KRBB; HSF1 inhibitor), rapamycin (Rap; mTOR inhibitor), and dorsomorphin (Dor; AMPK inhibitor). The inhibitors were also added to cells without MG132 (MG-). Total RNA was extracted after 24 hours and subjected to qPCR applying primers specific for Hpa2. Note that Hpa2 induction by MG132 is attenuated by inhibitors of AMPK and HSF1 (red arrows). C. Quantitation of Hpa2 induction by MG132 without or with KRIBB 11 (upper panel) and dorsomorphin (middle panel). Hpa2 expression is similarly decreased following silencing of HSF and AMPK-beta (C, lower panel). D. Hpa2 cells are more sensitive to stress conditions. Control (Vo) and Hpa2 overexpressing MKN-45 cells were treated with MG132 (20 μM) for the time indicated. Cell extracts were then prepared and subjected to immunoblotting applying antibodies directed against cleaved caspase 3 (upper panel), cleaved PARP (second panel) and tubulin (lower panel). Note increased levels of the apoptotic markers in Hpa2 cells.

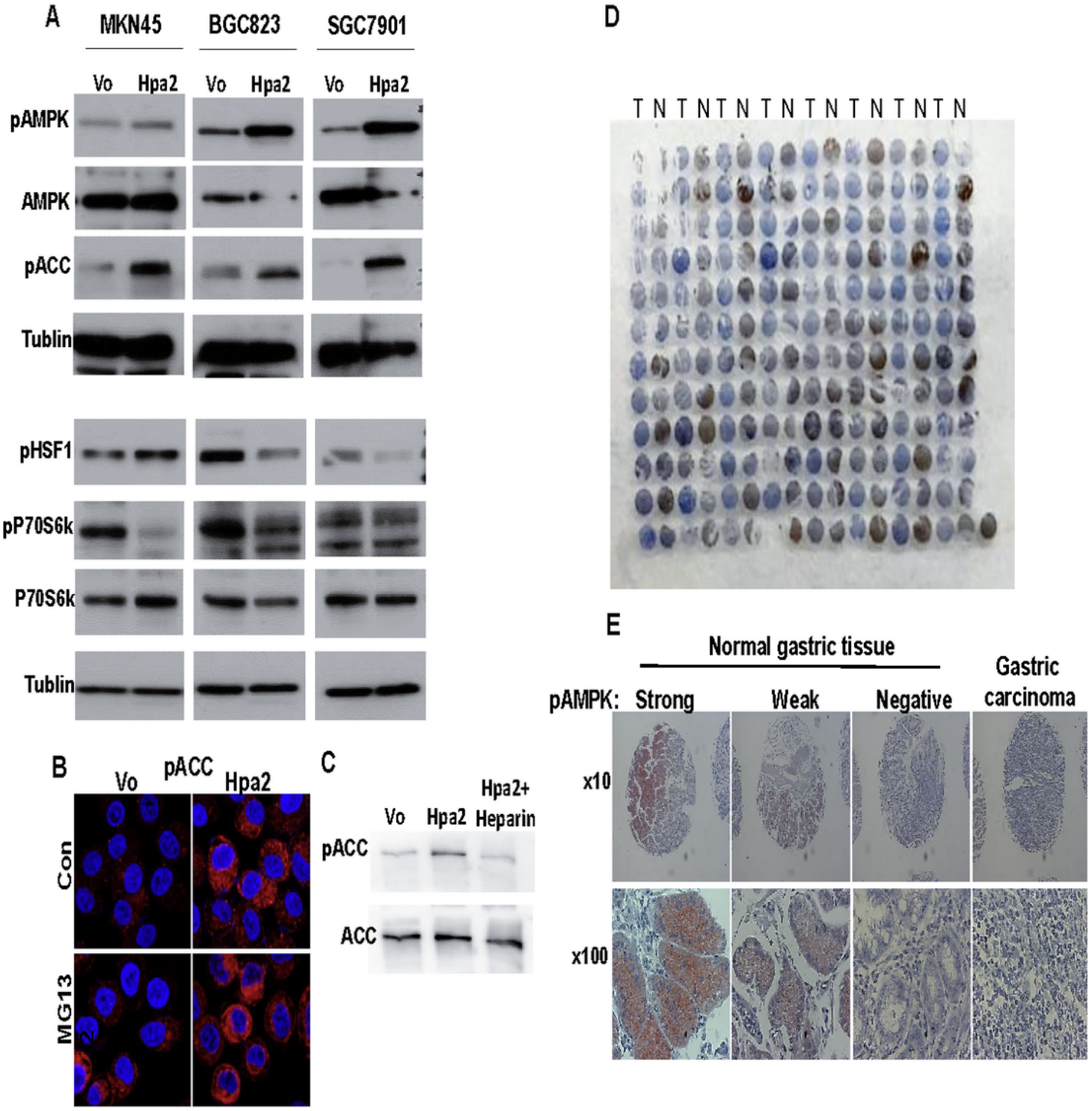

Figure 5

Increased AMPK phosphorylation in cells overexpressing Hpa2. A. Lysate samples of control (Vo) and Hpa2 overexpressing MKN-45 (left panels), BGC-823 (middle panels), and SGC-7901 (right panels) cells were subjected to immunoblotting applying the indicated antibody. B. Immunofluorescent staining. Control (Vo) and Hpa2 overexpressing SGC-7901 cells were treated with vehicle (Con) or MG132 (20 μM) for 16 hours. Cells were then fixed with cold methanol for 10 minutes and subjected to

immunofluorescent staining with anti-phospho-ACC antibody (red). Shown are representative images together with nuclear counter-staining (blue). Note stronger staining in Hpa2 cells before (upper right) and even more so after MG132 treatment (lower right) vs control (Vo) cells. C. Increased ACC phosphorylation by Hpa2 cells is HS-dependent. Hpa2 overexpressing SGC-7901 cells were left untreated or were treated with heparin (20 μM) added to the culture medium. Cell extracts were then prepared and subjected to immunoblotting applying anti-phospho-ACC (upper panel) and anti-ACC (lower panel) antibodies. D, E. AMPK phosphorylation is decreased in gastric cancer. A tissue array that includes biopsies of gastric carcinoma tumors (T) and adjacent normal gastric tissue (N) was subjected to immunostaining applying anti-phospho-AMPK antibody (D). Higher magnification of the staining in normal and tumor biopsies is shown in (E). Note decreased AMPK phosphorylation in tumor samples vs normal gastric tissue (see also Table 3).

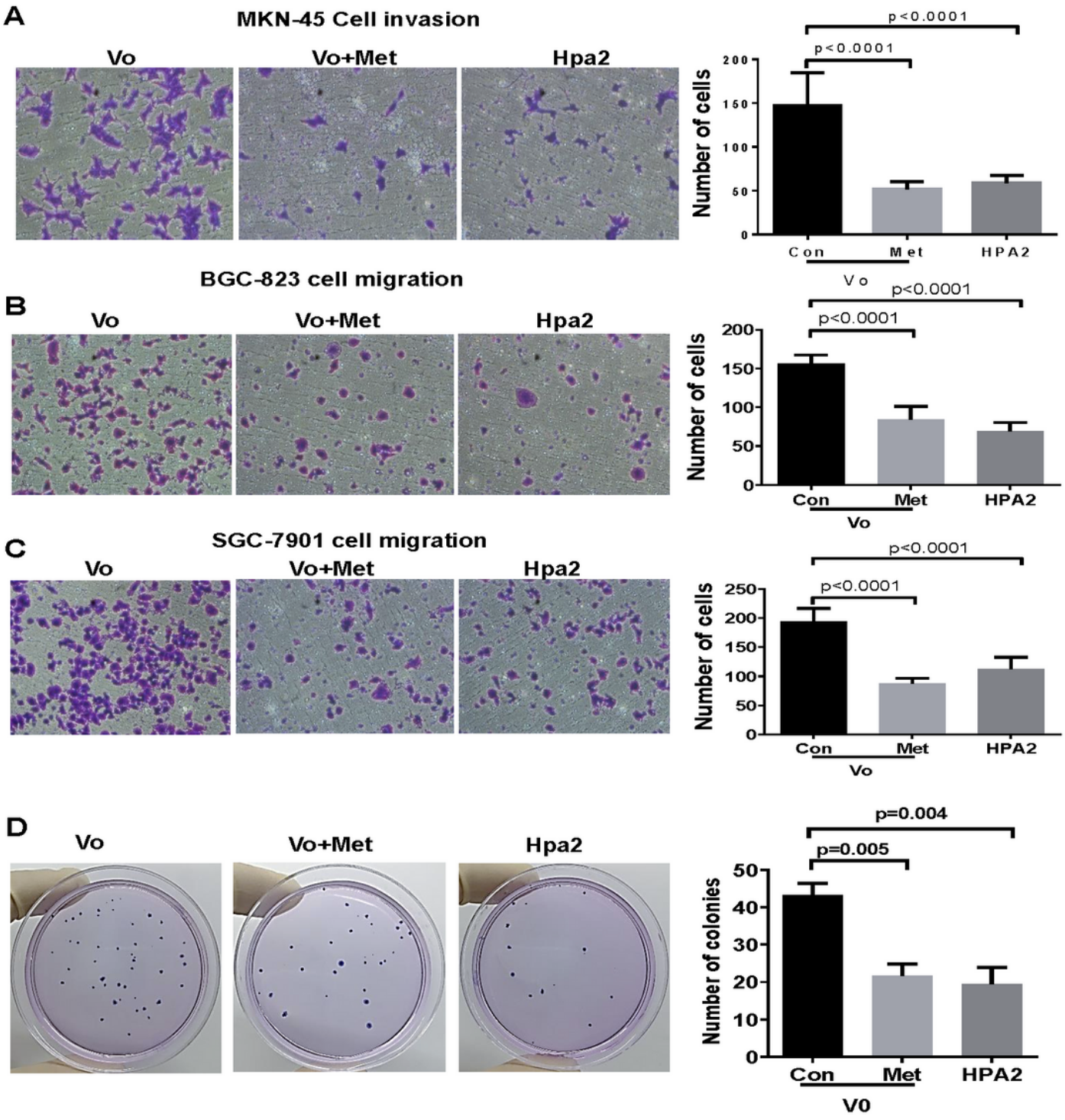

Figure 6

A-D. AMPK activation by metformin decreases the motility and colony formation by gastric carcinoma cells to levels comparable with Hpa2 overexpression. Cellular invasion and migration by control (Vo), Vo+metformin (0.5 mM), and Hpa2 overexpressing MKN-45 (A), BGC-823 (B), and SGC-7901 (C) cells were evaluated. Shown are representative images of invading (A) and migrating (B, C) cells taken 24 hours after cell seeding. Quantifications of the number of invading and migrating cells are shown

graphically in the right panels. Colony formation by BGC-823 cells untreated or treated with metformin, and overexpressing Hpa2 is shown in D. Quantification of colony number per dish is shown graphically at the right panel.

Supplementary Files

This is a list of supplementary files associated with this preprint. Click to download.

- Supplementaryfiles.pdf